

Detection of toxins-like peptides in plasma, urine and faecal samples from COVID-19 patients

Simone Cristoni^{1*+}, Carlo Brogna²⁺, Mauro Petrillo^{3*+}, Maddalena Querci³, Ornella Piazza⁴
and Guy Van den Eede⁵.

⁺ *The authors have equally contributed.*

1. ISB Ion Source & Biotechnologies srl, Bresso, Italy
2. Craniomed group srl. Montemiletto, Italy
3. European Commission, Joint Research Centre (JRC), Ispra, Italy
4. Department of Medicine and Surgery University of Salerno, Baronissi, Italy
5. European Commission, Joint Research Centre (JRC), Geel, Belgium

Short title: CIMS in COVID-19 metabolism investigation

Keywords: SANIST, CIMS, SANIST-CIMS, SARS-CoV-2, Covid-19

Corresponding authors:

Simone Cristoni

Via Ludovico Ariosto, 21

20091 Bresso (MI), Italy

Phone: +39-02-80887134

E-mail: simone.cristoni@isbiolab.com

Mauro Petrillo

Via E. Fermi, 2749

21027 Ispra (VA), Italy

Phone: +39-0332-786232

E-mail: mauro.petrillo@ec.europa.eu

Abstract

RATIONALE: SARS-CoV-2 virus that causes COVID-19 disease and led to the pandemic currently affecting the world has been broadly investigated. Different studies have been performed to understand the infection mechanism and the involved human genes, transcripts and proteins. In parallel, numerous clinical extra-pulmonary manifestations co-occurring with COVID-19 disease have been reported and evidence of their severity and persistence is increasing. Whether these manifestations are linked to other disorders co-occurring with SARS-CoV-2 infection, is under discussion. In this work, we report the identification of toxin-like peptides in COVID-19 patients by application of the SANIST-Cloud Ion Mobility Mass Spectrometry (SANIST-CIMS) technology.

METHODS: Plasma, urine and faecal samples from COVID-19 patients and control individuals were analysed to study toxins profiles. SANIST-CIMS instrumental parameters were selected to discriminate the ion cloud containing low and high molecular weight compounds. SANIST-Disc module was employed to investigate the differentially expressed molecules.

RESULTS: Toxin-like peptides, almost identical to toxic components of venoms from animals like conotoxins, phospholipase A2, phospholipase A1, activating prothrombotic factors, phosphodiesterases, zinc metal proteinases, and bradykinins, have been identified. As they were found only in samples from COVID-19 patients, their presence is considered somehow connected to SARS-CoV-2 infection. The presence of these peptides can potentially explain a large set of heterogeneous extra-pulmonary COVID-19 clinical manifestations, like myalgia, headache, encephalopathy, dizziness, dysgeusia, and anosmia. Even if the presence of each individual symptom is not selective of the disease, their combination could be related to COVID-19 in the presence of the panel of detected toxin-like peptides.

CONCLUSIONS: The data reported here suggest an association between COVID-19 disease and the release in the body of (oligo-)peptides almost identical to toxic components of venoms from animals. The presence of these peptides opens new scenarios on the aetiology of the COVID-19 clinical symptoms observed up to now, including neurological manifestations.

Introduction

Numerous clinical extra-pulmonary manifestations co-occurring with COVID-19 disease have been reported (as e.g. neurological, haemorrhagic, and thrombotic ones) and evidence of their severity and persistence is increasing. Gupta et al. reviewed the extrapulmonary organ-specific pathophysiology of patients with COVID-19, *'to aid clinicians and scientists in recognizing and monitoring the spectrum of manifestations, and in developing research priorities and therapeutic strategies for all organ systems involved'*¹. Liotta et al. have characterized the incidence of neurological manifestations in a cohort of hospitalised patients with confirmed COVID-19: the most frequent were myalgia, headache, encephalopathy, dizziness, dysgeusia, and anosmia; encephalopathy was found to be *'associated with increased morbidity and mortality, independent of respiratory disease severity'*². Whether these manifestations are linked to disorders co-occurring with SARS-CoV-2 infection is under discussion, including their concomitant occurrence, which could be strongly related COVID-19 disease. Frontera et al., by conducting a prospective, multi-centre, observational study of hospitalised adults with laboratory-confirmed SARS-CoV-2 infection, concluded that *'neurologic disorders were detected in 13.5% of COVID-19 patients during the study timeframe. Many of these neurologic disorders occur commonly among patients with critical illness. Encephalitis, meningitis or myelitis referable to SARS-CoV-2 infection did not occur, though post-infectious Guillain-Barre syndrome was identified. Overall, neurologic disorders in the context of SARS-CoV-2 infection confer a higher risk of in-hospital mortality and reduced likelihood of discharge home'*³.

Studies on the use of mass spectrometry in COVID-19 context focus on the search for augmented human inflammatory molecules to be used as biomarkers to assess the severity status of COVID-19 (see for example the work⁴ of Messner and colleagues). Our intent was to use the high sensitivity of SANIST- Cloud Ion Mobility Mass Spectrometry (SANIST-CIMS)^{5,6} to discover the eventual presence of molecules suggested by the clinical description of neurological, coagulation and inflammatory symptoms. SANIST-CIMS exhibits a high selectivity in peptide detection thanks to its ability to selectively isolate peptide ions through an in-source ion mobility (IM) effect. The mass spectra chemical noise is also strongly reduced due to the lower amounts of solvent cluster ions that are produced in low voltage ionization conditions. Thus, the peptide detection efficiency is strongly increased by the IM selectivity and lower chemical noise with respect to the classical high voltage ionization approaches. Therefore, our approach

started from the described clinical manifestations of COVID-19 (such as hyposmia, dysgeusia, etc.).

Here we present the results of our analyses. By using SANIST-CIMS, we found toxin-like peptides in plasma, urine and faecal samples from COVID-19 patients, but not in control samples. As our findings do not correspond with current thinking of the aetiology related to the observed clinical manifestations in COVID-19 patients, we feel their immediate sharing with the scientific community is critical.

Materials and Methods

Chemicals

NH₄HCO₃, methanol, acetonitrile and formic acid were purchased from Sigma-Aldrich (Milan, Italy). Bi-distilled water was purchased from VWR (Milan, Italy).

Cohort

Samples used in the present study: plasma samples collected from 15 COVID-19 patients from different cities of Italy and from 5 control individuals (i.e. negative to SARS-CoV-2 tests and not affected by cancer or autoimmune diseases); urine samples collected from 2 additional COVID-19 patients and from 2 control individuals; stool samples from 3 COVID-19 patients and from 3 control individuals. The human biological samples used in the experimentation were collected with the expressed consent, free and informed, to the collection and use, of the person from whom the material was taken, according to current legislation.

Sample preparation

Plasma

Each plasma sample was treated as follows: 5 µL of CH₃CN were added to 50 µL of plasma and vortexed for 1 minute. The procedure was repeated 10 times. Then the sample was centrifuged at 1,500 g for 10 minutes and two 100 µL aliquots of supernatant were dried and resuspended in 70 µL of NH₄HCO₃ 50 mmol. The solution was analysed by means of liquid chromatography (LC) coupled to SANIST-CIMS technology (LC-SANIST-CIMS).

Urine

Each urine sample was treated as follows: an equivalent volume of bi-distilled water was added, followed by centrifugation at 1,500 g for 10 minutes. 100 µL were dried and

resuspended in 70 μL of NH_4HCO_3 50 mmol. The sample was analysed by LC-SANIST-CIMS.

Stool

Each stool sample was treated as described by Cristoni et al.⁷ and analysed by LC-SANIST-CIMS.

Liquid chromatography

The Ultimate 3000 UPLC LC (by ThermoFisher) was used to achieve separation of analytes for each sample prior to MS analysis. A reversed phase Kinetex C-18 LC column (50×2.1 mm; particle size, 5 μm ; pore size, 100 Å, by Phenomenex, USA) was used. The eluent flow was 0.25 mL/min and the injection volume was 15 μL . The mobile phases were:

- A. 0.2% (v/v) formic acid (HCOOH);
- B. acetonitrile (CH_3CN).

The elution gradient was: 2% (v/v) of B between 0 and 2 min; 2 to 30% between 2 and 7 min; 30 to 80% between 7 and 9 min; 80% between 9 and 12 min; 80-2% between 12 and 12.1 min. The column was rebalanced with 2% of B between 12.1 and 17 min.

Mass spectrometry

All samples were analysed for the presence of proteins with potential toxic effect by using the SANIST-CIMS as described in literature^{5,6}. Samples were analysed with an ORBITRAP mass spectrometer (Breme, Germany) coupled to a surface activated chemical ionization (SACI) / ESI source and operated in positive ion mode. Full scan spectra were acquired in the 40-3,500 m/z range for non-targeted metabolomics/proteomics analyses to detect analytes. The same m/z range was used for both discovery studies and selective biomarker studies in order to standardize the instrument response across the SANIST study, primarily in terms of scan rate.

The ion source parameters were: ESI capillary voltage: 1,500 V; SACI surface voltage: 47 V; Desiccant gas: 2 L / min; Nebulizer gas: 80 psi; Temperature: 40 °C.

Mass spectrometry on samples was performed with collision-induced dissociation using data dependent scan and helium as the collision gas. The ion trap was applied to isolate and fragment the precursor ions (windows of isolation, ± 0.3 m/z ; collision energy, 30% of its maximum value, which was 5V peak to peak), and the ORBITRAP mass

analyser was used to obtain fragments with an extremely accurate m/z ratio (resolution 15,000; m/z error <10 ppm).

Data elaboration

The complete *UniprotKB set of manually reviewed venom proteins and toxins*⁸, mixed with a subset of not venom proteins and toxins from UniprotKB⁹ in order to give a statistical significance to the results, was used as reference protein dataset.

At the time of writing, TBLASTN¹⁰ was run at the National Center for Biotechnology Information (NCBI) website¹¹ with default options and parameters, with the exception of the following ones: max target sequences = 1,000; expect threshold = 100; word size = 3; gap cost existence = 9; gap cost extension = 1; filter of low complexity regions = No. Searches have been performed versus: Nucleotide collection (nr/nt); Reference RNA sequences (refseq_rna); RefSeq Genome Database (refseq_genomes); Whole-genome shotgun contigs (wgs) from metagenomic experiments; Sequence Read Archive (SRA) sequences from metagenomic experiments; Transcriptome Shotgun Assembly (TSA); Patent sequences(pat); Human RefSeqGene sequences (RefSeq_Gene); Betacoronavirus Genbank sequence dataset.

The information reported in Table 1 has been retrieved from the UniprotKB⁹ database and from the NCBI Taxonomy database¹², after confirmation by BLAST sequence comparison analysis¹⁰.

SANIST platform was optimized to perform the database search considering all potential protein points and post-translational modifications. No enzyme cutting rules were specified but all the protein subsequence combinations were taken into account. Database search calculation was performed by means of General Processing Graphic Processing Units (GPGPU).

The MS data are available upon request.

Results and discussion

Figure 1 reports (a) base peak LC- Full Scan (MS), tandem mass (MS/MS) chromatogram of an extracted plasma sample of a patient and a control subject and (b) a blow-up of a specific chromatogram region (5.713 – 5.719 min). The blow-up graph (Figure 1b) shows the four steps of data acquisition: 1) Full scan mass spectrum originated by the cloud containing low m/z ratio molecular species; 2) Tandem mass spectra (MS/MS) mass spectrum originated by the cloud containing low m/z ratio molecular species, 3) Full scan mass spectrum originated by the cloud containing medium-high (MedHigh) m/z ratio molecular species and 4) Tandem mass spectra (MS/MS) mass spectrum originated by the cloud containing (MedHigh) m/z ratio molecular species. The separation of low and medium-high m/z ratios makes it possible to reduce the ion trap saturation leading to maximize the detectable ion and the fragment ion list obtained during the data dependent scan. Positive LC-SANIST-CIMS analyses show the presence of high abundant signals in patients and not in the controls.

The presence of (oligo-)peptides characterised as toxic components of animal venoms was observed in plasma and urine samples from SARS-CoV-2 infected patients and never in plasma, urine and faecal samples from control individuals. Several (oligo-)peptides (between 70 and 115, depending on the analysed sample) matched to different animal venom proteins and toxins like conotoxins, phospholipases A2, metalloproteinases (86% of assignments have a $-\log(e)$ higher than 25). The protein list together with the peptide sequence and the MS/MS spectra exhibiting the sequence fragment matching are reported in supplementary material (Figure S1 – S6). Each protein was identified with a $-\log(e)$ higher than 25 (Table 2). In all case false discovery rate is exhibits a probability lower than 0.05 (Table 2).

A list of 36 proteins covered by the toxin-like peptides found is reported in Table 1. Examples of 5 spectra are reported in Figure 2a-e, and a selection of representative spectra is reported in Figure S1. Only mass spectra exhibiting a statistical $\log(e)$ score lower than -10 were considered for the identification. False discovery rate and statistical score were estimated by means of reverse sequence approach.

Some of the toxin-like peptides found mapped on the same reference protein (UniprotKB:D2DGD8), are reported in Figure 3: these peptides were found in the five plasma samples and in the three faecal samples.

The types of toxic-like peptides found resemble known conotoxins, phospholipases A2, metalloproteinases, prothrombin activators, coagulation factors, usually present in animal venoms, which are known to have high specificity and affinity towards human ion

channels, receptors and transporters of the nervous system, like the nicotinic acetylcholine receptor.

The same results have been observed on an additional set 10 plasma samples from 10 different patients. This matrix receives the peptides directly from the intestinal absorption and could be used as confirmation test matrix.

What follows is our attempt to elaborate a potential relation between their presence and extra-pulmonary COVID-19 symptomatology.

Conotoxins

Conotoxins are a group of neurotoxic peptides isolated from the venom of the marine cone snail of the genus *Conus*. Mature conotoxins consist of 10 to 30 amino acid residues and typically have one or more disulphide bonds. These disulphide patterns are used to define the structural classes of conotoxins (μ -conotoxins, ω -conotoxins, and α -conotoxins are the major classes). They are soluble in water and have a variety of mechanisms of actions, most of which have not yet been determined¹³. However, it has been shown that many of these peptides modulate the activity of several receptors, including ion channels, nicotinic acetylcholine receptors (nAChRs) and enzymes (acetylcholinesterases) that degrade acetylcholine, thus resulting in the alteration of acetylcholine levels and of cholinergic transmission^{14–16}. Regarding cholinesterases, the potential of cholinesterase levels and their interactions are significantly associated with severity and mortality in COVID-19 pneumonia patients¹⁷.

The presence of conotoxin-like peptides might explain the occurrence of many symptoms (like hyposmia, hypogeusia and the signs typical of Guillain-Barre syndrome) observed in some COVID-19 patients. Their presence can alter normal functioning of ion channels, nicotinic acetylcholine receptors and of acetylcholine levels.

Phospholipases A2

Phospholipases A2 (PLA₂, E.C. 3.1.1.4) hydrolyse phospholipids and lead to release of lysophosphatidic acid and arachidonic acid¹⁸. Arachidonic acid is a major precursor of many pro-inflammatory mediators like leukotriene, thromboxane and prostaglandin; as a consequence, abnormal presence of active PLA₂ can induce severe inflammation¹⁹. In animal venoms, PLA₂ act as neurotoxic proteins that bind to and hydrolyse membrane

phospholipids of the motor nerve terminal (and, in most cases, the plasma membrane of skeletal muscle) to cause a severe inflammatory degenerative response that leads to degeneration of the nerve terminal and skeletal muscle¹⁸. The drug dexamethasone is able to inhibit the prostaglandins synthesis and leukotriene formation²⁰. As dexamethasone is still the only therapeutic shown to be effective against the novel coronavirus in patients²¹ with severe symptoms, it can be that the positive effect of this drug on COVID-19 patients is also due to the reduction of the here identified PLA₂-like peptides.

Metalloproteinases

The last example of identified toxin-like peptides is about those recognised as metalloproteinases present in animal venoms, zinc-dependent enzymes of varying molecular weights having multidomain organization. These toxic enzymes cause haemorrhage, local myonecrosis, skin damage, and inflammatory reaction²². It has been reported that symptomatic COVID-19 patients have significantly lower zinc levels in comparison to controls and that zinc deficient patients develop more complications²³. The presence of this specific group of toxin-like peptides, which capture zinc, can be one of the reasons for such significantly low zinc levels in symptomatic COVID-19 patients.

Similarity searches by TBLASTN¹⁰ with relaxed parameters at the National Center for Biotechnology Information (NCBI) website (see Materials and Methods) revealed (in addition to mRNA sequences from the animal species reported in Table 1) almost identical short stretches (up to 10 amino acids) of these peptides in potential coding regions of many bacterial and viral sequences, but no long potential coding frame entirely covering any of them was found. Consequently, at the time of writing we have not yet identified the "genetic source" of these peptides, which could be:

- The SARS-CoV-2 RNA genome with its protein reading set, as proposed by Brogna²⁴, who reported the identification in SARS-CoV-2 RNA of many regions encoding for oligopeptides (four - five amino acids long) identical to neurotoxin peptides typical of animal venoms.
- The SARS-CoV-2 genome directly read by bacteria, assuming that SARS-CoV-2 genome, or parts thereof, is capable of replicating with a possible 'bacteriophage-like' mode of action, as previously described²⁵.
- Genomes of bacteria, which, as a reaction to the presence of the virus, secrete these peptides. This could happen by using still not well known and debated mechanisms, like alternative reading due to rRNA sequence heterogeneity (as described in²⁶⁻²⁷), or

the involvement of small bacterial ncRNA (sRNAs), known to be important regulators of gene expression under specific conditions (like stress response, quorum sensing, and virulence; Coleman et al., in 1984 described the first evidence of a functional sRNA of bacterial origin with the characterization of *micF* non-coding RNA²⁸).

- A combination of the above: e.g. the ‘toxin’ genetic code is present in the bacteria and expression may be triggered by SARS-CoV-2, acting like temperate bacteriophages, which are known to interact with bacteria so that they express (or not) certain genes, as described by Carey et al²⁹.

A detailed 3D structural similarity analysis between the toxin-like peptides found and reference proteins has not yet been conducted. Accordingly, at the time of writing, we can only speculate that these toxin-like peptides are involved in the clinical extra-pulmonary manifestations in symptomatic COVID-19 patients. According to our knowledge, these toxin-like peptides have never been searched in animals considered reservoirs of SARS-CoVs.

Conclusions

The presence (oligo-)peptides almost identical to toxic components of venoms from animals has been observed. Data and results reported here suggest an association between COVID-19 disease and the release in the body of these toxin-like peptides, and raise a series of questions:

- Are these finding in line with what proposed by Tizabi et al.³⁰, i.e. a potential therapeutic role for nicotine, nicotinic agonists, or positive allosteric modulators of nicotinic cholinergic receptors in COVID-19?
- If induced by SARS-CoV-2, can the production of toxin-like peptides be involved in the neurological disorders and injuries observed in hospitalized COVID-19 patients?
- If induced by SARS-CoV-2, can the production of toxin-like peptides influence complex diseases apparently triggered or enhanced by COVID-19, like e.g. Guillain-Barré Syndrome³¹ or Parkinson's disease³²?
- Are toxin-like peptides associated to SARS-CoV-2 infection or to other viral infections or, more in general, is their presence related to sickness condition?

- Are our findings supporting the suggestion made by the iVAMP Consortium³³ on the relationships between animal venom glands and microorganisms' microenvironments?

We consider that the immediate sharing of these results can contribute to the untangling of the multifaceted set of clinical manifestations in symptomatic COVID-19 patients, and to the further understanding of the mechanisms involved.

Acknowledgements

The author thanks Martina Larini and Simone Madama for paper revision.

Declarations

The scientific output expressed does not imply a policy position of the European Commission. Neither the European Commission nor any person acting on behalf of the Commission is responsible for the use that might be made of this publication.

Investigators received approval from their institutional review boards (University of Salerno) to use deferred consent.

REFERENCES

1. Gupta A, Madhavan M V., Sehgal K, et al. Extrapulmonary manifestations of COVID-19. *Nat Med.* 2020;26(7):1017-1032. doi:10.1038/s41591-020-0968-3
2. Liotta EM, Batra A, Clark JR, et al. Frequent neurologic manifestations and encephalopathy-associated morbidity in Covid-19 patients. *Ann Clin Transl Neurol.* October 2020;acn3.51210. doi:10.1002/acn3.51210
3. Frontera JA, Sabadia S, Lalchan R, et al. A Prospective Study of Neurologic Disorders in Hospitalized COVID-19 Patients in New York City. *Neurology.* October 2020;10.1212/WNL.0000000000010979. doi:10.1212/WNL.0000000000010979
4. Messner CB, Demichev V, Wendisch D, et al. Ultra-High-Throughput Clinical Proteomics Reveals Classifiers of COVID-19 Infection. *Cell Syst.* 2020;11(1):11-24.e4. doi:10.1016/j.cels.2020.05.012
5. Arzoni A, Bernardi LR, Cristoni S. In-source cloud ion mobility mass spectrometry. *Rapid Commun Mass Spectrom.* 2015;29(7):690-694. doi:10.1002/rcm.7136
6. Cristoni S, Dusi G, Brambilla P, et al. SANIST: optimization of a technology for compound identification based on the European Union directive with applications in forensic, pharmaceutical and food analyses. *J Mass Spectrom.* 2017;52(1):16-21. doi:10.1002/jms.3895
7. Cristoni S, Rossi Bernardi L, Larini M, et al. Predicting and preventing intestinal dysbiosis on the basis of pharmacological gut microbiota metabolism. *Rapid Commun Mass Spectrom.* 2019;33(14):1221-1225. doi:10.1002/rcm.8461
8. UniprotKB. Animal toxin annotation project.
<https://www.uniprot.org/program/Toxins>. Accessed October 4, 2020.
9. UniProt: a worldwide hub of protein knowledge. *Nucleic Acids Res.* 2019;47(D1):D506-D515. doi:10.1093/nar/gky1049

10. Altschul SF, Gish W, Miller W, Myers EW, Lipman DJ. Basic local alignment search tool. *J Mol Biol.* 1990;215(3):403-410. doi:10.1016/S0022-2836(05)80360-2
11. Johnson M, Zaretskaya I, Raytselis Y, Merezuk Y, McGinnis S, Madden TL. NCBI BLAST: a better web interface. *Nucleic Acids Res.* 2008;36(Web Server):W5-W9. doi:10.1093/nar/gkn201
12. Schoch CL, Ciufo S, Domrachev M, et al. NCBI Taxonomy: a comprehensive update on curation, resources and tools. *Database.* 2020;2020. doi:10.1093/database/baaa062
13. Layer R, McIntosh J. Conotoxins: Therapeutic Potential and Application. *Mar Drugs.* 2006;4(3):119-142. doi:10.3390/md403119
14. Cestèle S. Molecular mechanisms of neurotoxin action on voltage-gated sodium channels. *Biochimie.* 2000;82(9-10):883-892. doi:10.1016/S0300-9084(00)01174-3
15. Lebbe E, Peigneur S, Wijesekara I, Tytgat J. Conotoxins Targeting Nicotinic Acetylcholine Receptors: An Overview. *Mar Drugs.* 2014;12(5):2970-3004. doi:10.3390/md12052970
16. Prasasty V, Radifar M, Istyastono E. Natural Peptides in Drug Discovery Targeting Acetylcholinesterase. *Molecules.* 2018;23(9):2344. doi:10.3390/molecules23092344
17. Nakajima K, Abe T, Saji R, et al. Serum cholinesterase associated with COVID-19 pneumonia severity and mortality. *J Infect.* August 2020. doi:10.1016/j.jinf.2020.08.021
18. Harris J, Scott-Davey T. Secreted Phospholipases A2 of Snake Venoms: Effects on the Peripheral Neuromuscular System with Comments on the Role of Phospholipases A2 in Disorders of the CNS and Their Uses in Industry. *Toxins (Basel).* 2013;5(12):2533-2571. doi:10.3390/toxins5122533
19. Teixeira C, Fernandes CM, Leiguez E, Chudzinski-Tavassi AM. Inflammation Induced by Platelet-Activating Viperid Snake Venoms: Perspectives on

- Thromboinflammation. *Front Immunol.* 2019;10. doi:10.3389/fimmu.2019.02082
20. Goppelt-Struebe M, Wolter D, Resch K. Glucocorticoids inhibit prostaglandin synthesis not only at the level of phospholipase A2 but also at the level of cyclooxygenase/PGE isomerase. *Br J Pharmacol.* 1989;98(4):1287-1295.
doi:10.1111/j.1476-5381.1989.tb12676.x
 21. RECOVERY Collaborative Group. Dexamethasone in Hospitalized Patients with Covid-19 — Preliminary Report. *N Engl J Med.* July 2020:NEJMoa2021436.
doi:10.1056/NEJMoa2021436
 22. Teixeira C de FP, Fernandes CM, Zuliani JP, Zamuner SF. Inflammatory effects of snake venom metalloproteinases. *Mem Inst Oswaldo Cruz.* 2005;100(suppl 1):181-184. doi:10.1590/S0074-02762005000900031
 23. Jothimani D, Kailasam E, Danielraj S, et al. COVID-19: Poor outcomes in patients with zinc deficiency. *Int J Infect Dis.* 2020;100:343-349.
doi:10.1016/j.ijid.2020.09.014
 24. Brogna C. *The Covid-19 Virus Double Pathogenic Mechanism. A New Perspective.*; 2020. doi:10.20944/preprints202004.0165.v2
 25. Petrillo M, Brogna C, Cristoni S, Querci M, Piazza O, Van den Eede G. Increase of SARS-CoV-2 RNA load in faecal samples prompts for rethinking of SARS-CoV-2 biology and COVID-19 epidemiology. October 2020.
doi:10.5281/ZENODO.4088208
 26. Lilleorg S, Reier K, Volõnkin P, Remme J, Liiv A. Phenotypic effects of paralogous ribosomal proteins bL31A and bL31B in *E. coli*. *Sci Rep.* 2020;10(1):11682.
doi:10.1038/s41598-020-68582-2
 27. Chen Y-X, Xu Z-Y, Ge X, et al. Selective translation by alternative bacterial ribosomes. *Proc Natl Acad Sci U S A.* 2020;117(32):19487-19496.
doi:10.1073/pnas.2009607117

28. Coleman J, Green PJ, Inouye M. The use of RNAs complementary to specific mRNAs to regulate the expression of individual bacterial genes. *Cell*. 1984;37(2):429-436. doi:10.1016/0092-8674(84)90373-8
29. Carey JN, Metttert EL, Fishman-Engel DR, Roggiani M, Kiley PJ, Goulian M. Phage integration alters the respiratory strategy of its host. *Elife*. 2019;8. doi:10.7554/eLife.49081
30. Tizabi Y, Getachew B, Copeland RL, Aschner M. Nicotine and the nicotinic cholinergic system in COVID-19. *FEBS J*. 2020;287(17):3656-3663. doi:10.1111/febs.15521
31. Toscano G, Palmerini F, Ravaglia S, et al. Guillain–Barré Syndrome Associated with SARS-CoV-2. *N Engl J Med*. 2020;382(26):2574-2576. doi:10.1056/NEJMc2009191
32. Pavel A, Murray DK, Stoessl AJ. COVID-19 and selective vulnerability to Parkinson’s disease. *Lancet Neurol*. 2020;19(9):719. doi:10.1016/S1474-4422(20)30269-6
33. Ul-Hasan S, Rodríguez-Román E, Reitzel AM, et al. The emerging field of venom-microbiomics for exploring venom as a microenvironment, and the corresponding Initiative for Venom Associated Microbes and Parasites (iVAMP). *Toxicon X*. 2019;4:100016. doi:10.1016/j.toxcx.2019.100016

Table 1. Overview of candidate proteins on which toxin-like peptides have been mapped.

Thirty-six candidate protein sequences on which the identified toxin-like peptides have been mapped are here reported, together with information retrieved from UniprotKB and Taxonomy databases. The table is split in three sections according to the phylum of the reported species: *Chordata* (green), *Echinodermata* (pink), *Mollusca* (azure).

UNIPROTKB CANDIDATE'S INFORMATION							TAXONOMY CANDIDATE'S INFORMATION			
AC	ID	Status	Protein name	ENZYME EC	Other name(s)	Length (aa)	ID	Species	Phylum - Family	Organism's common name(s)
Q8AY46	VKTHB_BUNCA	reviewed	Kunitz-type serine protease inhibitor homolog beta-bungarotoxin B1 chain	NA	-	85	92438	<i>Bungarus candidus</i>	Chordata - Elapidae	Malayan krait
A6MEY4	PA2B_BUNFA	reviewed	Basic phospholipase A2 BFPA	EC 3.1.1.4	Antimicrobial phospholipase A2 Phosphatidylcholine 2-acylhydrolase (svPLA2)	145	8613	<i>Bungarus fasciatus</i>	Chordata - Elapidae	Banded krait Pseudoboa fasciata
F5CPF1	PA235_MICAT	reviewed	Phospholipase A2 MALT0035C	EC 3.1.1.4	Phospholipase A2 MALT0035C (svPLA2)	142	129457	<i>Micrurus altirostris</i>	Chordata - Elapidae	Uruguayan coral snake Elaps altirostris
A8QL59	VM3_NAJAT	reviewed	Zinc metalloproteinase -disintegrin-like NaMP	EC 3.4.24.-	Snake venom metalloproteinase (SVMPP)	621	8656	<i>Naja atra</i>	Chordata - Elapidae	Chinese cobra
Q9I900	PA2AD_NAJSP	reviewed	Acidic phospholipase A2 D	EC 3.1.1.4	svPLA2 APLA Phosphatidylcholine 2-acylhydrolase	146	33626	<i>Naja sputatrix</i>	Chordata - Elapidae	Malayan spitting cobra Naja naja sputatrix
Q58L90	FA5V_OXYMI	reviewed	Venom prothrombin activator omicarin-C non-catalytic subunit	NA	vPA Venom coagulation factor Va-like protein <i>Cleaved into 2 chains</i>	1460	111177	<i>Oxyuranus microlepidotus</i>	Chordata - Elapidae	Inland taipan Diemenia microlepidota
Q58L91	FA5V_OXYSU	reviewed	Venom prothrombin activator oscutarin-C non-catalytic subunit	NA	vPA Venom coagulation factor Va-like protein <i>Cleaved into 2 chains</i>	1459	8668	<i>Oxyuranus scutellatus</i>	Chordata - Elapidae	Coastal taipan
Q9W7J9	3S34_PSETE	reviewed	Short neurotoxin 4	NA	-SNTX4 Alpha-neurotoxin 4	79	8673	<i>Pseudonaja textilis</i>	Chordata - Elapidae	Eastern brown snake
P23028	PA2AD_PSETE	reviewed	Acidic phospholipase A2 homolog textilotoxin D chain	NA	svPLA2 homolog	152	8673	<i>Pseudonaja textilis</i>	Chordata - Elapidae	Eastern brown snake
Q593B6	FA5_PSETE	reviewed	Coagulation factor V	NA	<i>Cleaved into 2 chains</i>	1459	8673	<i>Pseudonaja textilis</i>	Chordata - Elapidae	Eastern brown snake
Q75ZNO	FA5V_PSETE	reviewed	Venom prothrombin activator pseutarin-C non-catalytic subunit	NA	PCNS vPA Venom coagulation factor Va-like protein <i>Cleaved into 2 chains</i>	1460	8673	<i>Pseudonaja textilis</i>	Chordata - Elapidae	Eastern brown snake
Q2XXQ3	CRVP1_PSEPL	reviewed	Cysteine-rich venom protein ENH1	NA	CRVP Cysteine-rich secretory protein ENH1 (CRISP-ENH1)	239	338839	<i>Pseudoferania polylepis</i>	Chordata - Homalopsidae	Macleay's water snake Enhidris polylepis
Q9PW56	BNP2_BOTJA	reviewed	Bradykinin -potentiating and C-type natriuretic peptides	NA	Brain BPP-CNP Evasin-CNP <i>Cleaved into the 12 chains</i>	265	8724	<i>Bothrops jararaca</i>	Chordata - Viperidae	Jararaca
A8YPR6	SVM1_ECHOC	reviewed	Snake venom metalloprotease inhibitor	NA	O2D01 O2E11 I0F07 Smp1-Eoc7 <i>Cleaved into 15 chains</i>	308	99586	<i>Echis ocellatus</i>	Chordata - Viperidae	Ocellated saw-scaled viper
Q698K8	VM2L4_GLOBR	reviewed	Zinc metalloproteinase /disintegrin [Fragment]	EC 3.4.24.-	<i>Cleaved into 3 chains</i>	319	259325	<i>Gloydius brevicaudus</i>	Chordata - Viperidae	Korean slamosa snake Agkistrodon halys brevicaudus
Q8AWI5	VM3HA_GLOHA	reviewed	Zinc metalloproteinase -disintegrin-like halysase	EC 3.4.24.-	Zinc metalloproteinase-disintegrin-like halysase Snake venom metalloproteinase (SVMPP) Vascular apoptosis-inducing protein (VAP)	610	8714	<i>Gloydius halys</i>	Chordata - Viperidae	Chinese water mocassin Agkistrodon halys
P82662	3L26_OPHHA	reviewed	Alpha- neurotoxin	NA	Alpha-elapitoxin-Oh2b (Alpha-EPTX-Oh2b) Alpha-elapitoxin-Oh2b LNTX3 Long neurotoxin OH-6A/OH-6B OH-3	91	8665	<i>Ophiophagus hannah</i>	Chordata - Viperidae	King cobra Naja hannah
Q2PG83	PA2A_PROEL	reviewed	Acidic phospholipase A2 PePLA2	EC 3.1.1.4	Phosphatidylcholine 2-acylhydrolase (svPLA2)	138	88086	<i>Protobothrops elegans</i>	Chordata - Viperidae	Elegant pitviper Trimeresurus elegans
P06860	PA2BX_PROFL	reviewed	Basic phospholipase A2 PL-X	EC 3.1.1.4	Phosphatidylcholine 2-acylhydrolase (svPLA2)	122	88087	<i>Protobothrops flavoviridis</i>	Chordata - Viperidae	Habu Trimeresurus flavoviridis
P0C7P5	BNP_PROFL	reviewed	Bradykinin -potentiating and C-type natriuretic peptides	NA	BPP-CNP <i>Cleaved into 6 chains</i>	193	88087	<i>Protobothrops flavoviridis</i>	Chordata - Viperidae	Habu Trimeresurus flavoviridis
Q3C2C2	PA21_ACAPL	reviewed	Phospholipase A2 AP-PLA2-I	EC 3.1.1.4	Phosphatidylcholine 2-acylhydrolase (svPLA2)	159	133434	<i>Acanthaster planci</i>	Echinodermata - Acanthasteridae	Crown-of-thorns starfish
D6C4M3	CU96_CONCL	reviewed	Conotoxin C19.6	NA	Conotoxin C19.6	81	1736779	<i>Californiconus californicus</i>	Mollusca - Conidae	California cone Conus californicus
D2Y488	VKT1A_CONCL	reviewed	Kunitz-type serine protease inhibitor conotoxin Cal9.1a	NA	-	78	1736779	<i>Californiconus californicus</i>	Mollusca - Conidae	California cone Conus californicus
D6C4J8	CUE9_CONCL	reviewed	Conotoxin C114.9	NA	-	78	1736779	<i>Californiconus californicus</i>	Mollusca - Conidae	California cone Conus californicus
P0DPT2	CA18_CONCT	reviewed	Alpha- conotoxin C1B [Fragment]	NA	C1.2	41	101291	<i>Conus catus</i>	Mollusca - Conidae	Cat cone
V5V893	CQG3_CONFL	reviewed	Conotoxin Fla16d	NA	Conotoxin Fla16d <i>Cleaved into 2 chains</i>	76	101302	<i>Conus flavidus</i>	Mollusca - Conidae	Yellow Pacific cone
P58924	CS8A_CONGE	reviewed	Sigma- conotoxin GVIIIA	NA	Sigma-conotoxin GVIIIA	88	6491	<i>Conus geographus</i>	Mollusca - Conidae	Geography cone Nubecula geographus
P0DM19	NF2_CONMR	reviewed	Conotoxin Mr15.2	NA	Conotoxin Mr15.2 (Mr094)	92	42752	<i>Conus marmoreus</i>	Mollusca - Conidae	Marble cone
P0C1N5	M3G_CONMR	reviewed	Conotoxin mr3g	NA	Conotoxin mr3g (Mr3.6)	68	42752	<i>Conus marmoreus</i>	Mollusca - Conidae	Marble cone
D2DGD8	I361_CONPL	reviewed	Conotoxin Pu6.1	NA	-	83	93154	<i>Conus pulicarius</i>	Mollusca - Conidae	Flea-bite cone
P0C8U9	CA15_CONPL	reviewed	Alpha- conotoxin -like Pu1.5	NA	-	81	93154	<i>Conus pulicarius</i>	Mollusca - Conidae	Flea-bite cone
A1X8B8	CA1_CONQU	reviewed	Putative alpha- conotoxin Qc alphaL-1	NA	Qcal-1	68	101313	<i>Conus quercinus</i>	Mollusca - Conidae	Oak cone
P58786	COW_CONRA	reviewed	Contryphan -R	NA	Bromocontryphan <i>Cleaved into 2chains</i>	63	61198	<i>Conus radiatus</i>	Mollusca - Conidae	Rayed cone
P58811	CA1A_CONTU	reviewed	Rho- conotoxin TIA	NA	Rho-TIA	58	6495	<i>Conus tulipa</i>	Mollusca - Conidae	Fish-hunting cone snail Tulip cone
Q5K0C5	O16A_CONVR	reviewed	Conotoxin 10	NA	-	79	89427	<i>Conus virgo</i>	Mollusca - Conidae	Virgin cone
B3FIA5	CVFA_CONVR	reviewed	Conotoxin Vi15a	NA	Conotoxin Vi15.1	74	8765	<i>Conus virgo</i>	Mollusca - Conidae	Virgin cone

Table 2. List of proteins and the related $-\log(e)$ and false discovery ratio (FDR) expressed as pvalue.

Protein	ID	Database	$-\log(e)$	FDR pvalue
Conotoxin Pu6.1	D2DGD8	Uniprot	75	0.001
Conotoxin Vi15a	B3FIA5	Uniprot	89	0.005
Putative alpha-conotoxin Qc alphaL-1	A1X8B8	Uniprot	76	0.005
Conotoxin 10	Q5K0C5	Uniprot	76	0.001
Rho-conotoxin TIA	P58811	Uniprot	54	0.001
Kunitz-type serine protease inhibitor conotoxin Cal9.1a	D2Y488	Uniprot	67	0.001
Alpha-conotoxin-like Pu1.5	P0C8U9	Uniprot	57	0.002
Conotoxin Fla16d	V5V893	Uniprot	67	0.003
Phospholipase A2 MALT0035C	F5CPF1	Uniprot	87	0.003
Phospholipase A2 AP-PLA2-I	Q3C2C2	Uniprot	81	0.004
Acidic phospholipase A2 PePLA2	Q2PG83	Uniprot	66	0.001
Basic phospholipase A2 BFPA	A6MEY4	Uniprot	69	0.001
Basic phospholipase A2 PL-X	P06860	Uniprot	70	0.001
Complement factor B Ba fragment	Q91900	Uniprot	74	0.001
Acidic phospholipase A2 homolog textilotoxin D chain	P23028-1	Uniprot	73	0.002
Acidic phospholipase A2 homolog textilotoxin D chain	P23028-2	Uniprot	65	0.002
Venom prothrombin activator pseutarin-C non-catalytic subunit	Q7SZN0	Uniprot	60	0.002
Coagulation factor V	Q593B6	Uniprot	61	
Venom prothrombin activator oscutarin-C non-catalytic subunit	Q58L91	Uniprot	87	0.001
Short neurotoxin 4	Q9W7J9	Uniprot	69	0.001
Conotoxin Cl9.6	D6C4M3	Uniprot	58	0.002

Zinc metalloproteinase-disintegrin-like halysase	Q8AWI5	Uniprot	57	0.003
Alpha-elapitoxin-Oh2b	P82662	Uniprot	96	0.003
Sigma-conotoxin GVIIIA	P58924	Uniprot	43	0.002
Conotoxin Mr15.2	P0DM19	Uniprot	47	0.001
Conotoxin mr3g	P0C1N5	Uniprot	74	0.001
Contryphan-R	P58786	Uniprot	58	0.002
Snake venom metalloprotease inhibitor 02D01	A8YPR6	Uniprot	43	0.002
Bradykinin-potentiating and C-type natriuretic peptides	P0C7P5	Uniprot	51	0.003
Bradykinin-potentiating and C-type natriuretic peptides	Q9PW56	Uniprot	51	0.003
Zinc metalloproteinase/disintegrin	Q698K8	Uniprot	49	0.004

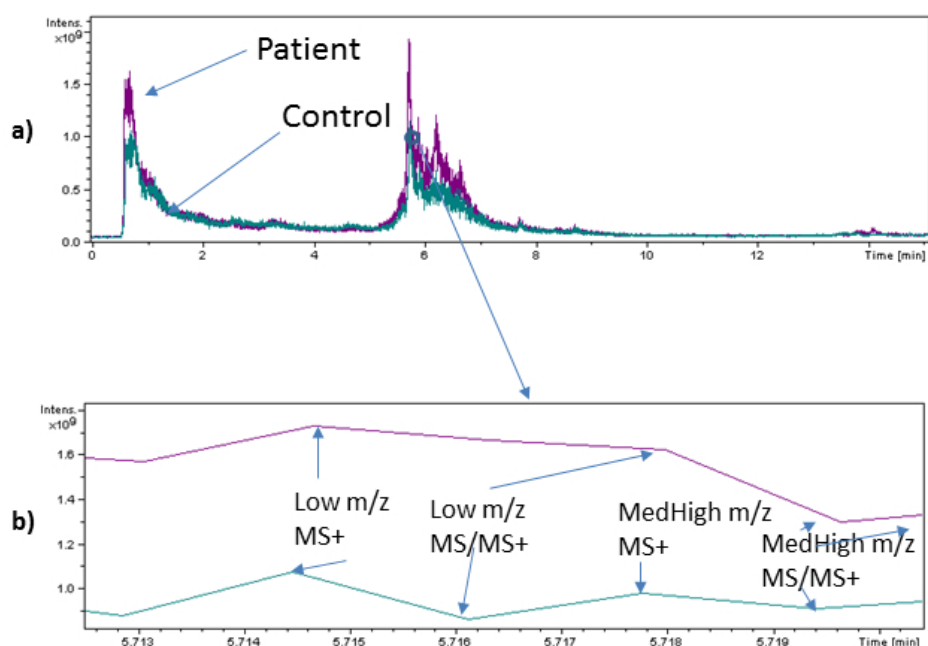
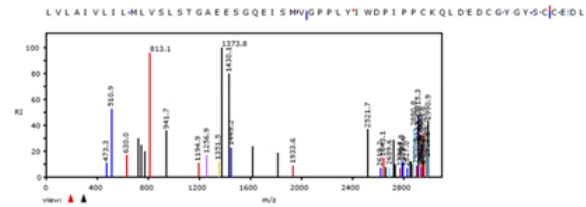


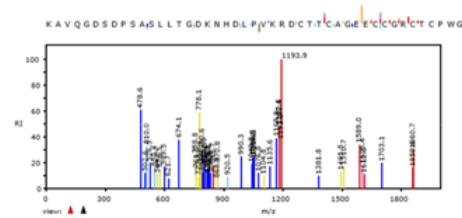
Figure 1

(a) Base peak LC- Full Scan (MS), tandem mass (MS/MS) chromatogram of an extracted plasma sample of a patient and a control subject and (b) a blow-up of a specific chromatogram region (5.713 – 5.719 min). The blow-up shows the four regions of data acquisition: 1) Full scan mass spectrum originated by the cloud containing low m/z ratio molecular species; 2) Tandem mass spectra (MS/MS) mass spectrum originated by the cloud containing low m/z ratio molecular species; 3) Full scan mass spectrum originated by the cloud containing medium-high (MedHigh) m/z ratio molecular species; 4) Tandem mass spectra (MS/MS) mass spectrum originated by the cloud containing medium-high (MedHigh) m/z ratio molecular species.

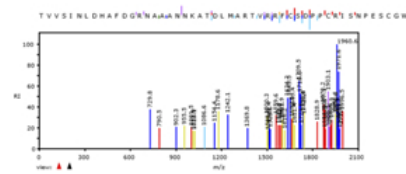
a) D2DGD8



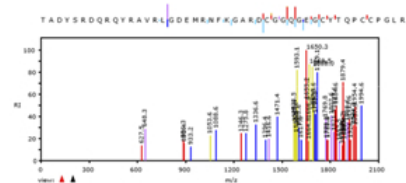
b) B3FIA5



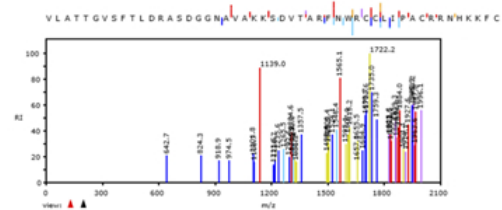
c) A1X8B8



d) Q5K0C5



e) P58811



D2DGD8 - I361_CONFL Conotoxin Pu6.1 (*Conus pulicarius*)

D2DGD8 **MKLVLAIVLILMLVSLSTGAEE****SGQEISMVGPP****LYIWDPIPP****CKQLDEDCGYGYSCCEDLSCQPLIEPDTMEITALVCQIESA**

PS01.01 [01] MKLVLAIVLILMLVSLSTGAEE**SGQEISMVGPP**LYIWDPIPPCKQLDEDCGYGYSCCEDLSCQPLIEPDTMEITALVC-----
 PS01.02 [01] MKLVLAIVLILMLVSLSTGAEE**SGQEISMVGPP**LYIWDPIPPCKQLDEDCGYGYSCCEDLSCQPLIEPDTMEITALVCQI---
 PS01.03 [02] --LVLAIVLILMLVSLSTGAEE**SGQEISMVGPP**LYIWDPIPPCKQLDEDCGYGYSCCEDLSCQPLIEPDTMEITALVCQI---
 PS01.04 [30] --LVLAIVLILMLVSLSTGAEE**SGQEISMVGPP**LYIWDPIPPCKQLDEDCGYGYSCCEDLSCQPLIEPDTMEITALVCQIES-
 PS02.01 [01] MKLVLAIVLILMLVSLSTGAEE**SGQEISMVGPP**LYIWDPIPPCKQLDEDCGYGYSCCEDLSCQPLIEPDTMEITALVCQIES-
 PS02.02 [01] -KLVAIVLILMLVSLSTGAEE**SGQEISMVGPP**LYIWDPIPPCKQLDEDCGYGYSCCEDLSCQPLIEPDTMEITALVCQIESA
 PS02.03 [31] --LVLAIVLILMLVSLSTGAEE**SGQEISMVGPP**LYIWDPIPPCKQLDEDCGYGYSCCEDLSCQPLIEPDTMEITALVCQIESA
 PS03.01 [01] ----LAIVLILMLVSLSTGAEE**SGQEISMVGPP**LYIWDPIPPCKQLDEDCGYGYSCCEDLSCQPLIEPDTMEITALVCQIESA
 PS03.02 [11] --LVLAIVLILMLVSLSTGAEE**SGQEISMVGPP**LYIWDPIPPCKQLDEDCGYGYSCCEDLSCQPLIEPDTMEITALVCQIESA
 PS04.01 [01] -KLVAIVLILMLVSLSTGAEE**SGQEISMVGPP**LYIWDPIPPCKQLDEDCGYGYSCCEDLSCQPLIEPDTMEITALVCQIESA

Figure 3

Alignment of the toxin-like peptides to Conotoxin Pu6.1. Conotoxin Pu6.1 from *Conus pulicarius* (UniprotKB:D2DGD8) is aligned with the toxin-like peptides identified in four out of five plasma samples. Being the protein secreted and cleaved, leader-region pro-peptide and mature cysteine rich domains are highlighted in green, yellow and red, respectively. Each identified toxin-like peptide is named according to the sample of origin and its uniqueness. For each of them, the number reported in square brackets indicates the number of identical toxin-like peptides identified in the same sample.